PHYS 4430 Final Report: Diffusion with Pulsed Nuclear Magnetic Resonance

Kyle Moe

April 28, 2022

1 Abstract

In this experiment, we attempted to use NMR to find the diffusion coefficients, D, of liquids with distinct properties using the TeachSpin NMR apparatus and permanent magnet. By using resonance to map the magnetic field gradient, we could measure signal decay to make accurate measurements of the spin-spin relaxation time (T_2) with the Carr-Purcell Meiboom-Gill (CPMG) pulse sequence in regions of near zero gradient. By modifying parameters, we measured decay in regions of known gradient to generate values of the diffusion coefficient D. This procedure was then repeated with the different liquids to draw conclusions about the effect of material's properties. As anticipated, we found long T_2 values for small molecules with large tumbling rates such as water. For more complex molecules, like mineral oil, we saw two short T_2's requiring the need to account for a bieponential as opposed to the expected single decay rate. This can be justified by examinations of the power spectrum of the decay. These T_2 values allowed for calculations of diffusion coefficients which broadly were in accordance with measured values and our expectations from the material's molecular properties.

2 Introduction

Though NMR affects all nuclei with a non-zero intrinsic spin, our foremost concern will be with the isolated protons within ^1H nuclei. Each of these protons are spin-1/2, giving rise to a magnetic moment that, when placed into a magnetic field, will assume one of two distinct energy levels U,

$$U = -\vec{\mu} \cdot \vec{B} = \pm \frac{\gamma \hbar B_0}{2} \tag{1}$$

separated by an energy ΔU:

$$\Delta U = \gamma \hbar B_0 = \hbar \omega_0 \tag{2}$$

written in terms of frequency $\omega_0 = \gamma B_0$.

Magnetic resonance comes from the fact that if we apply a signal to these protons with the frequency ω_0, we can raise those protons from the lower energy state to the higher-energy state. The way the TeachSpin apparatus goes about applying this 'torque' is through a circularly polarized field, orthogonal to B_0, that is tuned to this resonance frequency. When on the resonance frequency, this magnetization (while continuing to precess around the background field B_0) will precess about this applied field. If when turned off, the magnetization is oriented exclusively in the transverse (x-y) plane, we call it a $\pi/2$-pulse. Likewise, if anti-aligned with the background B_0, it is called a π-pulse.

In our experiment, we will be examining the decay of the transverse magnetization after a $\pi/2$-pulse. This requires using the CPMG [1] pulse sequence consisting of an initial $\pi/2$-pulse followed by a number of π-pulses. This sequence prevents spin-lattice relaxation back toward B_0 and eliminates the effect of magnetic field inhomogeneities as spins in different environments re-cohere into an echo. Such a sequence allows us to measure the characteristic time associated with this decay, T_2.

However, there exists a complication in using this pulse sequence that Carr and Purcell were aware of when first outlining the sequence in [2]. That is the effect of diffusion. If the proton is able to move to a region of a different magnetic field, it will not re-cohere with the bulk of protons at the time of the spin-echo and thus its contribution to the magnetization will be reduced. Assuming that each particle makes a random walk within a discrete time step, Carr and Purcell derived the following equation to account for this diffusion of particles that is based on the development of a normal distribution of accumulated phase differences for each particle in the sample.

$$M_{x,y}(t) = M_0 e^{-\frac{t}{T_2} - \frac{\gamma^2 (\frac{\partial B_{0,z}}{\partial x,y})^2 D t^3}{12 n^2}} \tag{3}$$

It is with this formula that we will be able to solve for the diffusion coefficient D.

3 Experimental Methods

3.1 TeachSpin Apparatus

As described above, the primary method of taking measurements is through the CPMG pulse sequence. This method accounts for both measuring T_2 and D and as such, we could simply modify the parameters defining the sequence and the environment in which the sample is placed to examine the desired phenomenon. Depending on the need to either suppress diffusive effects or allow such affects to be prominent, we either programmed high n pulse sequences or low n (often $n = 1$) sequences respectively. Additionally, we also placed the sample into regions of small magnetic field gradient to reduce diffusion's effect and placed it in a region of a well defined field so diffusion's effect was more prominent and we could then measure D.

Fortunately most of the tools necessary to perform such pulse sequences were provided by the TeachSpin Pulsed NMR Apparatus. This includes a pulse programmer module from which we can define the total number of π-pulses and their separation in time. These programmed pulses

are then sent to the transmitter coil (placed in the x-y plane) that bounds our sample within its housing in the permanent magnet. This is shown below in Figure 1. Additionally, the TeachSpin

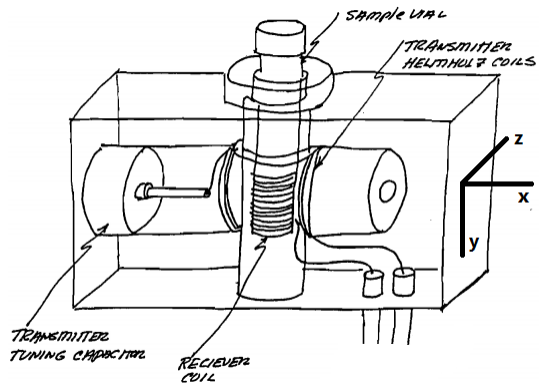

Figure 1: Diagram of sample housing within permanent magnet [3]

apparatus has an LCD display that allows us to a tune the transmitter's tuning capacitor to a known numerical frequency near 15MHz. The sample within the housing will respond according to the theory of NMR and, depending on the frequency of these applied pulses, the receiver coil (also in the x-y plane), then picks up the induced emf from the oscillating spins. This signal is then sent to our oscilloscope for us to view the free-induction decay of our sample. Conveniently, the TeachSpin apparatus also provides functionality to mix the frequencies from the pulse programmer with the frequencies picked up by the receiver coil so that we might view only the total net magnetization in the transverse plane.

The bulk of our measurements will be made by recording the maximum amplitude of the signals detected by the receiver coil. As these signals are output on to our oscilloscope, we can view the entirety of a CPMG pulse sequence and its corresponding signal responses after the different pulses. An example of this showing many π-pulses and the subsequent spin-echoes of the net magnetization is shown in Figure 2.

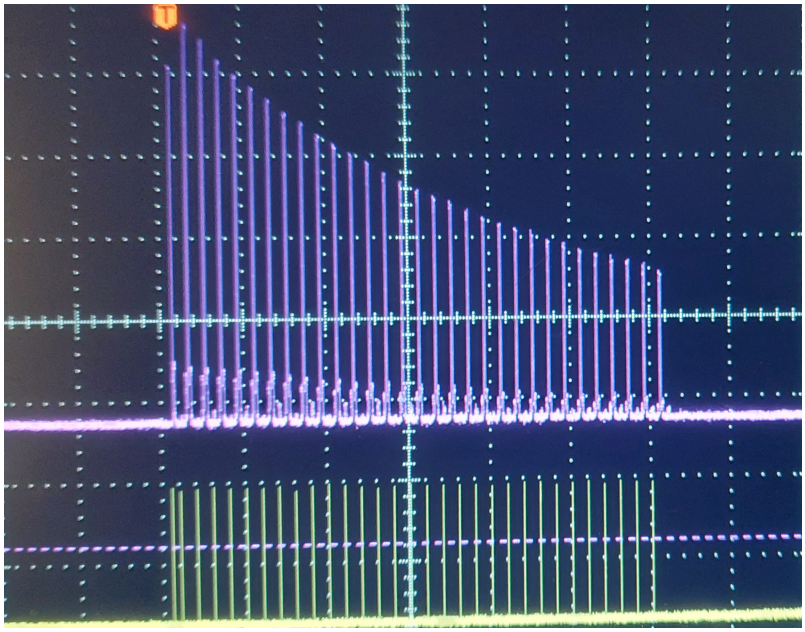

Figure 2: CPMG pulse sequence (yellow) and the spin-echoes (purple). Primary measurement is of voltage at peaks as this directly maps the spin-spin relaxation of the sample.

3.2 Measurement Methods

There are two primary measurements that were made in the course of this experiment. These were of the spin-spin relaxation time T_2 and the diffusion coefficient D, in that order. The methodology for making each of these measurements was informed primarily by the two terms in Equation 3. We begin our examination of each sample by attempting to determine its T_2. This, according to Equation 3, requires suppression of the second term within the exponential such that the reduction in the decay time on account of diffusion is minimized and we can conveniently model our decay by the sole exponential defined by T_2. This demands two considerations: how to increase the density of π-pulses within the CPMG pulse sequence and decrease the gradient of the background magnetic field into which the sample is placed.

For the latter of these two, we located a region within our permanent magnet that provided the closest approximation of a uniform magnetic field and used that region for all subsequent T_2 measurements. Dealing with how densely packed the π-pulses must be was a trickier, however. Water, with a high D, required delay times between pulses of no more than 0.25ms for accurate

measurements while with the thicker materials like mineral oil, we could comfortably use delay times of multiple milliseconds. The additional complication of the maximum 99 π-pulses also limited our ability to make accurate measurements for those samples with longer T_2. All of these measurements were made by recording the peaks of the FID signals, like what can be seen in Figure 2, and generating a fitting function from Equation 3 under the assumption that the diffusion term in the exponential goes to zero.

The next step in this procedure was to measure the diffusion coefficient D. This requires making use of the value for T_2 generated in the previous step and making modifications to both the gradient and the pulse sequence. To this end, we selected a region of near-linear gradient and made measurements of the magnetic field in this region, solving for the average gradient. All further diffusion coefficient measurements are then made in this region. For the pulse sequence, all that was required was a reduction in the density of our π-pulses and the recording of the new FID peaks from which a fit for D was produced. This again requires some consideration of the material as for thicker materials, the low diffusion values hardly show up with sequences of any more than a single π-pulse.

4 Results

While the foremost goal of this experiment was to determine those diffusion coefficients of our materials, this could not be done without first understanding the environment into which our samples would be placed. This requires knowing the background magnetic field at a given location and more importantly, the gradient of the magnetic field. Though not necessary, we elected to make an exhaustive mapping of the magnetic field throughout the permanent magnet. This would allow us to identify the regions where there is the most apparent uniformity in the magnetic field and those regions where a first-order approximation of our gradient seems most appropriate. The contour plot of the magnetic field is shown in Figure 3.

From this mapping of the magnetic field, we identified the approximate region of zero gradient

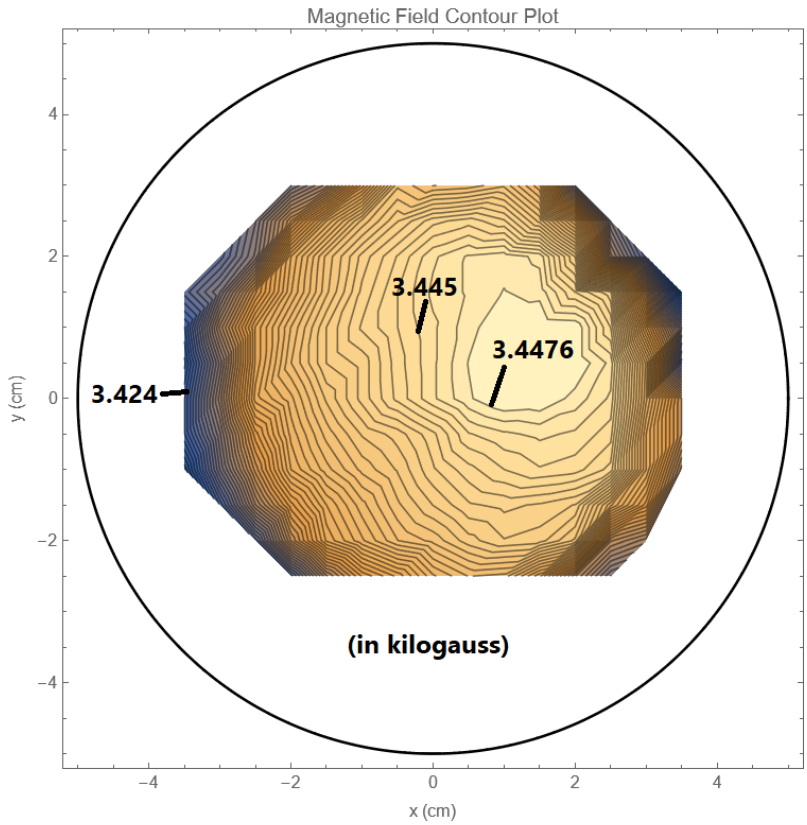

Figure 3: Contour plot of magnetic field within permanent magnet. Field measured by tuning transmission signal to resonance. Signal is lost at edges of contour.

to be contained within $x \in (1, 2)$ cm and $y \in (0, 1)$ cm. Likewise, we chose the region defined by $x \in (-1, 0)$ cm and $y \in (0, 1)$ cm to be the most appropriate to generate a linear gradient. The precise location chosen was at $(x, y) = (-0.25cm, 0.25cm)$ and at this location we calculated the gradient to be $\frac{\partial B_{0,z}}{\partial x,y} = 2.6 \pm 0.2\ gauss/cm$, a value used for all subsequent diffusion measurements

4.1 Measuring T_2

From this point, we were equipped to begin making measurements of the T_2 relaxation times. The samples were placed in the low-gradient region and the CPMG was applied to each in turn. What followed was a series of trial and error to try and adequately suppress the effect of diffusion. The delay time between π-pulses was reduced until there was no appreciable change in the measured T_2 generated by the fit. For materials of long T_2 and large D such as water

and isopropanol, we were challenged by the fact that we only had a maximum of 99 π-pulses. Making the delay time too small caused our error in T_2 to explode. As such, it is likely that our measurements of T_2 for these sort of materials is shorter than the true value. The decay for water and its corresponding T_2 is shown in Figure 4

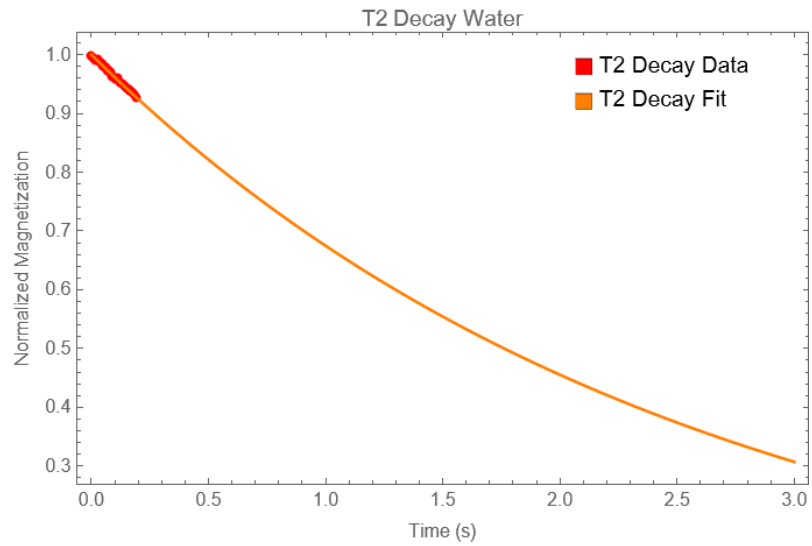

Figure 4: Decay of water where $T_2 = 2.58 \pm 0.03s$

There was an additional complication that was discovered when generating fits like that in Figure 4 for certain other materials. When attempting to fit for mineral oil, for instance, it was clear from simply looking at the attempted fit that a single exponential decay was inadequate at capturing the full structure of this sample's decay. What proved to be the effective remedy was modifying the decay of magnetization given by Equation 3 such that it would be given by a bi-exponential of two unique T_2 values. The correction to Equation 3 is given by Equation 4.

$$M_{x,y}(t) = (M_{0,1}e^{-\frac{t}{T_{2,1}}} + M_{0,2}e^{-\frac{t}{T_{2,2}}})e^{-\frac{\gamma^2(\frac{\partial B_{0,z}}{\partial x,y})^2 Dt^3}{12n^2}} \tag{4}$$

Again we assume that the diffusion term on the right is suppressed when fitting for each of these two unique T_2 values. By applying this new biexponetial model to the decays of both mineral oil and the 3-in-1 Household Oil, we were able to substantially reduce the residuals and covariance in our fits. Figure 5 shows the drastic effect of this change.

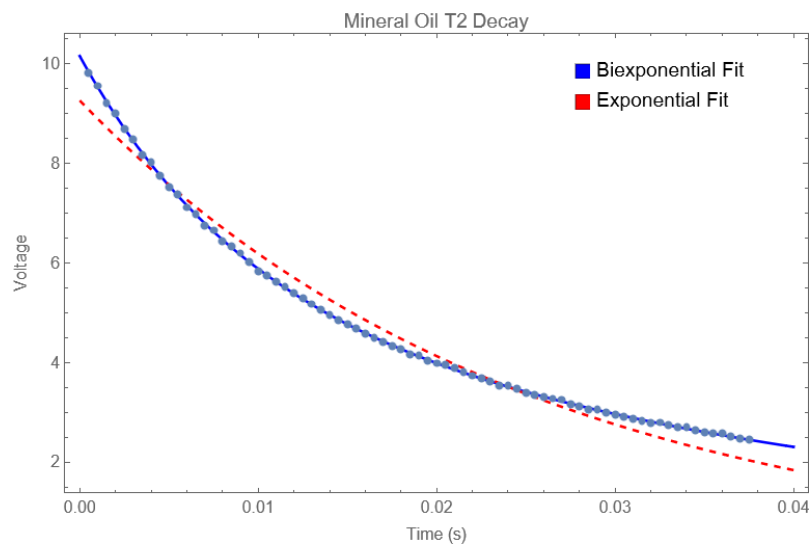

Figure 5: Decay of Mineral Oil where $T_{2,1} = 9.4 \pm 0.1ms$ and $T_{2,2} = 49.1 \pm 0.5ms$

With this change, we were equipped to find the relaxation times of the four materials that we examined. Both the mineral oil and 3-in-1 household oil samples were well fit by the new model given by Equation 4. As expected, because each of its two protons should experience the same environment, water remained well-described by Equation 3. Isopropanol is the only of our four materials that continued to have issues. From the fit generated using a single T_2 decay time, it appears that there may be covariance that is not captured by the model. However, because of the limitations in the number of π-pulses and the high diffusivity of isopropanol, we can't effectively capture additional decay rates without allowing decay due to diffusion to obscure any result. Thus, the data on T_2 values presented in Table 1 excludes isopropanol as it requires further investigation.

Sample	$T_{2,1}$	$T_{2,2}$
Water	2.58 ± 0.03 s	N/A
Mineral Oil	9.4 ± 0.1 ms	49.1 ± 0.5 ms
3 in 1 Household Oil	29 ± 1 ms	135 ± 5 ms

Table 1: T_2 measurements for Water, Light Mineral Oil, and 3 in 1 Household Oil with units (Isopropanol excluded)

The errors listed in Table 1 come from the standard deviation of the mean from repeated

trials that each yielded their own T_2 values and standard error within each material's respective fitting function.

Broadly, these results reflect expectations. T_2 is the measure of how quickly magnetic moments dis-align on account of interactions between nearby spins. Because water is such a small molecule relative to the other two, it experiences a much higher tumbling rate and the protons within the molecule often see these spin-spin interactions "average out." Thus it is not surprising that water's T_2 is longer as variations in local magnetic field on account of spin-spin interactions is largely minimized from this tumbling. Comparatively, larger molecules like the two oils tend to tumble at much slower rates. Additionally, the complexity of the molecules means that there is a subset of protons whose spins are always affecting the local field and usually from the same fixed distance. Even between the mineral oil and the 3 in 1 oil, the results reflect expectations. While only the mineral oil has an explicit chemical formula, the heavy napthenic oil that composes most of the 3 in 1 is generally lighter than the mineral oil. Thus it is reasonable to suspect that the 3 in 1 oil experiences greater tumbling and has fewer fixed protons than mineral oil, a suspicion that seems to be confirmed by the data in Table 1

4.2 Measuring D

Now, equipped with these values of T_2 we can make precision measurements of the diffusion coefficient D. First, our samples are placed into the region of defined gradient described at the top of the section. Next is to change the pulse sequence. For water, this simply requires increasing the delay time between the π-pulses and fitting to Equation 3, this time treating the diffusion term as non-zero and fixing the parameter T_2. From Figure 6 we can see just how stark the effect of diffusion is even with a small increase in the delay time. Additionally, we can clearly see the effectiveness of Equation 3 in describing the decay for a single exponential with diffusion considered.

The data for mineral oil and the 3 in 1 oil required a much smaller number of π-pulses, often

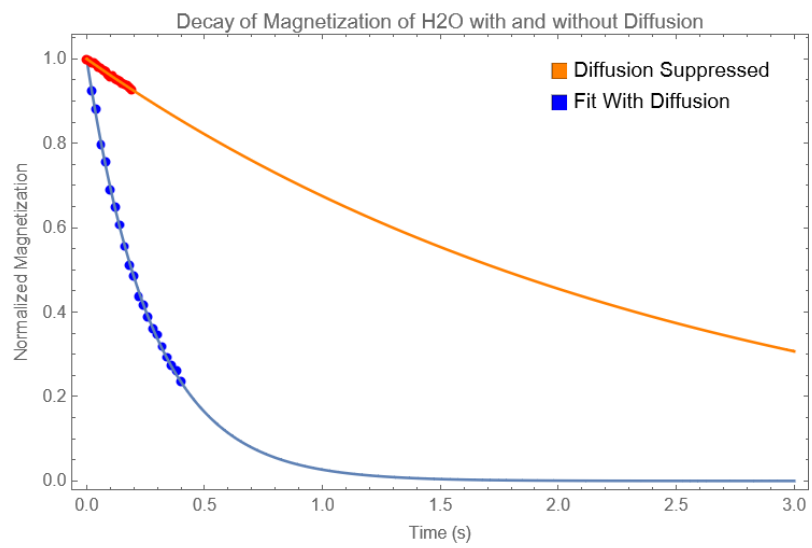

Figure 6: Decay of the magnetization water with and without diffusion suppressed. Yielded $D = (2.0 \pm 0.3) * 10^{-5} cm^2 s^{-1}$.

$n = 1$. But, like water, these still yielded the expected decays that were now clearly modeled by the biexponential provided by Equation 4. For each, we are able to see how these material's smaller diffusion terms (relative to water) meant that the differences between decays with and without diffusion are much smaller than that of water. For mineral oil in particular, for which both T_2 values are much smaller than those of the 3 in 1 oil, the we can see just how small the diffusion effect is.

Such similarities between the decays with and without diffusion highlight the difficulty in accurately collecting data that would allow us to generate reasonable values for the diffusion coefficient. The first of these challenges involved recognition of the necessity of the biexponential fit. This is because by assuming a single T_2 value, our data was almost always collected over delay time ranges that inadequately captured the full structure of the decay. We can see in the plots in Figure 7 that data points taken at large t were necessary to properly distinguish between the decays with and without diffusion effects. For instance, with mineral oil, the single exponential fit tended to give $T_2 \sim 25ms$ after which diffusion data was taken from 0 to about 40 ms. However, as one may suspect from the fact that one of the two T_2 values from the biexponential fit was $49.1 \pm 0.5ms$, this clearly would struggle at capturing structure at longer

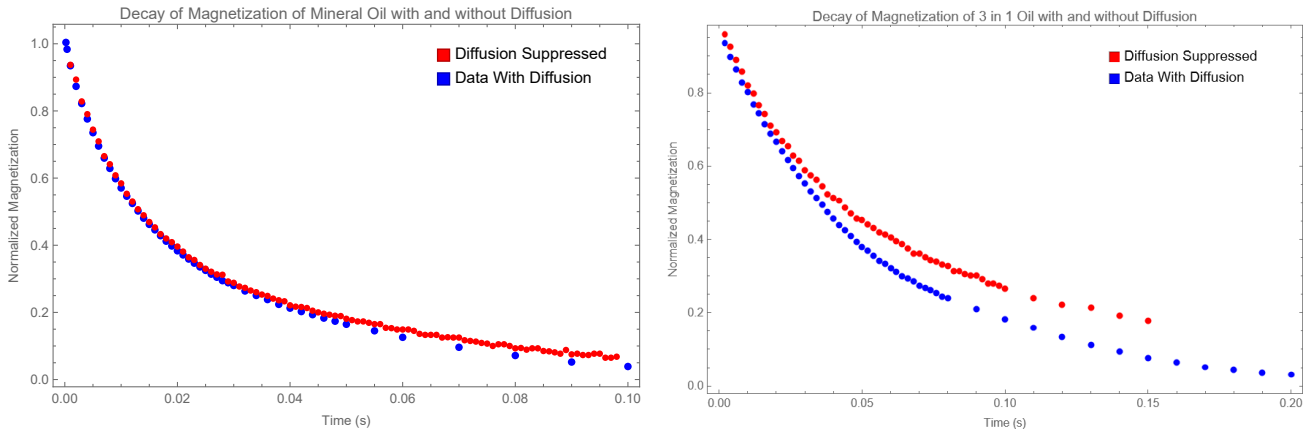

(a) Data for Mineral Oil

(b) Data for 3 in 1 Oil

Figure 7: T_2 decay with and without diffusion for mineral and household oils. Fits not included for due to clutter. (a) Comparison between the decays with and without diffusion effects for mineral oil. (b) Same comparison for 3 in 1 oil.

times.

A second issue arose from sparseness of data points. Both of the above plots show a high density of data points collected (at least at low t). This was necessary to counteract issues generated from statistical error that, as one would suspect, were more prevalent when fewer data points were taken of the decays. Increasing the density of the sampling reduced these errors and produced more consistent values for both T_2 values and those of D. Prior to making these two improvements to our sampling methods, the fits generate values for T_2 that fluctuated wildly and would often produce values of D for which the uncertainty was an order of magnitude larger than the actual value. For mineral oil and the household oil the value of D was just as likely to be negative as positive. However, once these issues were recognized, our measurements were more effective with much reduced error. The three values of the diffusion coefficient are summarized in Table 2.

These measurements reflect our expectations. At the temperature of $21°C$ in the lab, the diffusion coefficient for water matched well with those provided in [4]. Likewise, though we lacked explicit experimental calculations of the diffusion coefficients of mineral oil or the household oil, we did have prior knowledge of the general molecular sizes and viscosities found at [5] and [6].

Sample	D in cm^2s^{-1}
Water	$2.0 \pm 0.3 *10^{-5}$
Mineral Oil	$2.5 \pm 0.6 *10^{-7}$
3 in 1 Household Oil	$4.8 \pm 0.8 *10^{-7}$

Table 2: Diffusion coefficient (D) measurements for Water, Light Mineral Oil, and 3 in 1 Household Oil in units of cm^2s^{-1}.

All of these would suggest a slowly diffusing molecule with a low D, results that are clearly shown in the experimentally determined values.

The error quoted in the above table is the result of the propagation of our three known sources of uncertainty. The first of these, and often the most dominant source, was from the measurement of the magnetic field gradient. The two others come from the standard error generated by fitting for the T_2 value(s) and the similar fitting to the parameter D and arose from random error in our measurements. Repeated fits reduced the value of the latter two and the results in Table 2 reflect the combination of the three.

4.3 Mineral Oil NMR Spectroscopy

While the success that came from applying the biexponential fit itself provided justification for adopting such a model, we desired to find some additional grounds for its use. To this end, we turned toward NMR spectroscopy. Though applying this technique within the TeachSpin apparatus and permanent magnet is rudimentary at best, it proved none-the-less effective in identifying distinct structures within mineral oil that give rise to the two decay rates.

To perform this, we begin with the free-induction decay of the transverse magnetization. Up to this point, we have been exclusive using the envelope containing the net magnetization in the transverse plane for all measurements of the signal decays. For NMR spectroscopy, we instead wish to examine the oscillating magnetization of the magnetic moments themselves. This free-induction decay following a single $\pi/2$-pulse is shown in Figure 8.

The utility of this comes from the fact that we are able to apply a Fourier transform to this

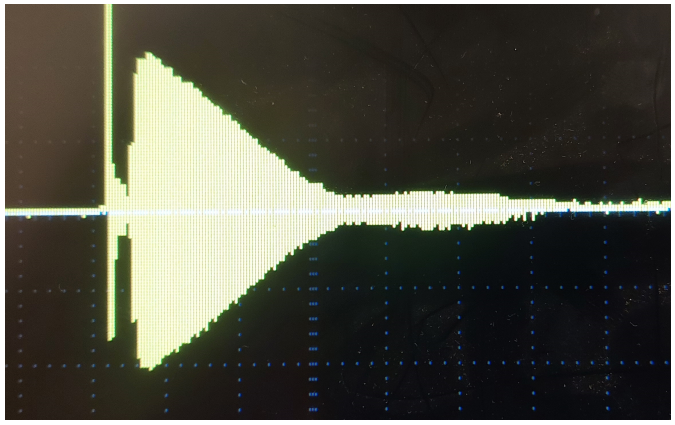

Figure 8: Free-Induction Decay (FID) of mineral oil

waveform to extract the resonance response frequencies of all the protons within the sample after the perturbation pulse is applied. In doing so, we may identify distinct resonance frequencies for subsets of the protons, suggesting different local environments and relaxation behavior.

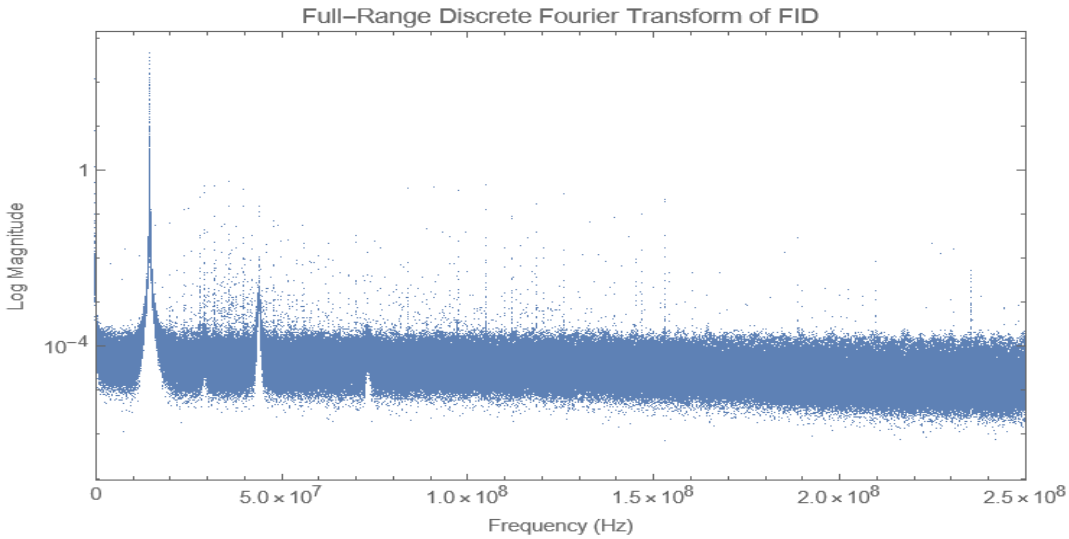

Figure 9: Full-range Discrete Fourier Transform of FID signal. Sampling Frequency = 500MHz, $N = 2 * 10^6$ samples.

Figure 9 shows the full range of the discrete Fourier transform of the free-induction decay. The expected resonance frequency characterizes the strongest peak at approximately 14.67MHz with peaks at harmonic frequencies, suggesting that there exists more than a single waveform at the resonance frequency. In order to determine whether this is the case, we need to zoom

in on the resonance frequency and look at the structure of its peak. This is shown in Figure 10(a). While there does appear to be structure within the main peak with what could be called a "bump" on the right side, it cannot be isolated largely due to broadening from the inhomogeneous magnetic field and the rapid decay rate (T_2^*) of the free-induction decay.

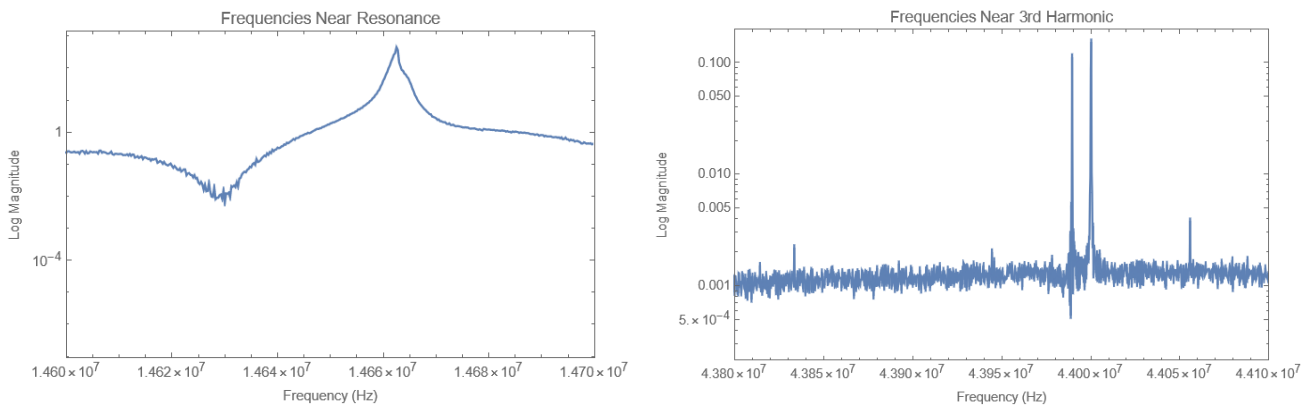

(a) Near resonance frequency of 14.67MHz

(b) Frequencies near 3rd harmonic

Figure 10: Power spectrum near 1st and 3rd harmonics. In (a) low point occurs at frequency where signal is lost (edge of contour plot in Figure 3). Signal broadened and structure obscured. In (b) tripling of resolution reveals distinct peaks.

This is where we take advantage of the 3rd harmonic. Because the harmonics ought to capture the same structures as the peak at the resonance frequency, we may examine their structure in the same way we might examine that of the resonance frequency. Except that now, every frequency is just three times the magnitude of the actual frequency. The benefit of this is that we get triple the resolution on the structure of the frequency responses. In Figure 10(b) we can see how this increase in resolution allows for two large peaks to become distinguishable. This alone tells us that within mineral oil, there exist no fewer than two unique magnetic field environments for protons within the molecule. While this is not enough to conclusively say that these different environment are the result of different spin-spin interactions experienced (as would be necessary to state that they must give rise to unique T_2 values), it does seem to provide sufficient justification for the biexponential fit.

It is also possible that we might identify which T_2 value each peak is likely to correspond to.

Because of magnetization signal is decaying, there is a natural broadening to each peak. The consequence of this is that the full-width half-maximum of each spectral line is proportional to $1/(\pi T_2^*)$ [7]. This should, theoretically, allow us to identify which peak matches with each T_2. Unfortunately, the lack of resolution means that, in our scenario, these FWHM values are nearly identical. As such we can't definitively say one way or another which decay rate corresponds to which peak.

5 Conclusion

This experiment demonstrated the utility of pulsed NMR in determining both relaxation times of samples as well as those sample's diffusion coefficients. For water, the spin-spin relaxation time was found to be $T_2 = 2.58 \pm 0.03s$. For more complex molecules, the spin-spin relaxation had to be modeled by a biexponential of two unique decay rates. For mineral oil, the measured relaxation rates were $T_{2,1} = 9.4 \pm 0.1ms$ and $T_{2,2} = 49.1 \pm 0.5ms$. And finally, for the 3 in 1 household oil, these relaxation rates were $T_{2,1} = 29 \pm 1ms$ and $T_{2,2} = 135 \pm 5ms$. These values then allowed us to find the diffusion coefficients of these materials. For water, this value was found to be $D = (2.0 \pm 0.3) * 10^{-5} cm^2 s^{-1}$ while for mineral oil and household oil, the diffusion coefficients were found to be $D = (2.5 \pm 0.6) * 10^{-7}$ and $D = (4.8 \pm 0.8) * 10^{-7}$ respectively. These conformed to expectations within the uncertainties provided by the magnetic field gradient and numerical fits, thus showing the effectiveness in this method of diffusion coefficient measurement for both simple and complex molecules.

References

[1] P. McIntosh L. CPMG. *Roberts G.C.K. (eds) Encyclopedia of Biophysics*, 2013. doi: 10.1007/978-3-642-16712-6_320.

[2] H. Y. Carr and E. M. Purcell. Effects of diffusion on free precession in nuclear magnetic resonance experiments. *Phys. Rev.*, 94:630–638, May 1954. doi:10.1103/PhysRev.94.630.

[3] Barbara Wolff-Reichert. A Conceptual Tour of TeachSpin's Pulsed NMR. Mar. 2003.

[4] Olaf Dietrich. Diffusion coefficients of water. https://dtrx.de/od/diff/, Oct 2002.

[5] Mineral Oil, Light (NF/FCC), Fisher Chemical. https://www.fishersci.com/shop/products/mineral-oil-light-nf-fcc-fisher-chemical-3/O1211.

[6] 3 in 1 Multi-Purpose Oil TDS. https://media.3inone.com/app/uploads/2021/12/03161614/3-IN-ONE-Multi-Purpose-Oil-Marksman-TDS-Sheet-7-23-21.pdf.

[7] Size and shape of peaks. https://mriquestions.com/sizeshapes-of-peaks.html.

6 Appendix

See GitHub for Code: https://github.com/kylemoe4/PersonalProjects/tree/main/DiffusionNMR